

Research Article

Reduction of Carbonaceous and Nitrogenous Disinfection Byproduct Precursors from Coagulated/Filtered Algae-laden Water: Comparison of Vacuum Ultraviolet and Ultraviolet Processes with and without Persulfate Activation

Somphong Soontharo, Panitan Jutaporn, Sumana Siripattanakul-Ratpukdi and Thunyalux Ratpukdi* Department of Environmental Engineering, Faculty of Engineering and Research Center for Environmental and Hazardous Substance Management, Khon Kaen University, Khon Kaen, Thailand

Pradabduang Kiattisaksiri

Faculty of Public Health, Thammasat University (Lampang Center), Lampang, Thailand

Eakalak Khan

Department of Civil and Environmental Engineering and Construction, University of Nevada, Las Vegas, Nevada, United States of America

* Corresponding author. E-mail: thunyalux@kku.ac.th DOI: 10.14416/j.asep.2025.10.006

Received: 14 July 2025; Revised: 15 August 2025; Accepted: 4 September 2025; Published online: 14 October 2025

© 2025 King Mongkut's University of Technology North Bangkok. All Rights Reserved.

Abstract

This study investigated reductions in carbonaceous and nitrogenous disinfection byproduct (DBP) precursors in algae-laden water using vacuum ultraviolet (VUV), VUV with persulfate (PS) (VUV/PS), ultraviolet (UV), and UV with PS (UV/PS) processes. The effect of PS doses (5 and 50 mg/L) on dissolved organic matter (DOM) removal was evaluated. DOM (as the DBP precursor) was measured using dissolved organic carbon (DOC), dissolved organic nitrogen (DON), and UV absorbance at 254 nm, as well as characterized by fluorescence excitation—emission matrix (EEM) spectroscopy. The results showed that the VUV/PS (PS dose of 50 mg/L) process was the most effective, removing 30%—46% DOC and 27% DON in 60 min. The EEM results revealed that the VUV/PS process reduced all fluorophores—including humic-like, fulvic-like, tyrosine protein-like, and tryptophan protein-like—by more than 88%. The DOC removal and fluorescence loss corresponded with the trihalomethane formation potential (THMFP) reductions. Chloroform and dichloroacetonitrile were the predominant species among THMFP and haloacetonitrile formation potential (HANFP), respectively. However, brominated DBPs, which are known to be more toxic than chlorinated DBPs, were also detected. These processes achieved greater THMFP reductions compared to the UV and UV/PS processes. Overall, the VUV and VUV/PS processes show potential for future application in enhancing the treatment of algae-laden water.

Keywords: Advanced oxidation processes, Algae, Excitation–emission matrix, Haloacetonitrile formation potential, Trihalomethane formation potential, Vacuum ultraviolet

1 Introduction

The global water shortage has become a significant international issue [1]. This situation necessitates the use of treated municipal wastewater or contaminated natural water as the raw water source for water supplies and drinking water. Such water sources are likely to contain nutrients, which can cause algal

blooms [2]. This increases the levels of algal organic matter (AOM) and algal toxins and can cause odor and taste issues [2], [3].

Water containing algae cells and AOM contains increased concentrations of dissolved organic carbon (DOC) and dissolved organic nitrogen (DON). During chlorine (Cl₂) disinfection in water treatment plants, DOC and DON react with Cl₂, producing carbonaceous



and nitrogenous disinfection byproducts (C-DBPs and N-DBPs), respectively. The predominant C-DBPs and N-DBPs in algae-laden water are trihalomethanes (THMs) and haloacetonitriles (HANs) [4], [5]. The World Health Organization (WHO) provides guideline values for common THMs and HANs found in drinking water, including chloroform (CF) (at 300 μg/L), dibromochloromethane (DBCM) (100 μg/L), bromodichloromethane (BDCM) (60 µg/L), bromoform (BF) (100 μg/L), dichloroacetonitrile (DCAN) (20 μg/L), and dibromoacetonitrile (DBAN) (70 μg/L). The types and concentrations of THMs (10.4–159.6) $\mu g/L$) and HANs (2-86 $\mu g/L$) found in treated water produced from algae-laden water vary and occasionally exceed permissible concentrations [6], [7]. In some cases, the presence of inorganic ions such as bromide could increase the formation of brominated DBPs (more toxic than chlorinated DBPs) upon chlorination of algae-laden water [5]. To control disinfection byproduct (DBP) formation, effective DOC and DON (as DBP precursors) removal technology is necessary.

The conventional water treatment process (coagulation/flocculation and filtration) has limitations for DOC and DON removal [8], [9]. While algal cells can be removed by coagulation, extracellular organic matter (EOM) can be released [10]. Ozone can oxidize EOM; however, the formation of bromate (an inorganic DBP) in the presence of bromide (>100 μ g/L) is an issue, as is the increase in brominated THMs (which are more toxic) when bromide exceeds 50 µg/L [4]. ultraviolet-based advanced oxidation Recently, processes (UV-AOPs) have become an effective alternative for removing contaminants, including DOC and DON in the presence of bromide $> 100 \mu g/L$ [7], [11]–[13]. Typically, low-pressure mercury ultraviolet (UV) lamps (emitting 254 nm) are used to disinfect drinking water. To degrade contaminants, oxidants such as hydrogen peroxide (H_2O_2) , ozone (O_3) , Cl_2 , and persulfate (S₂O₈²⁻)—can be added to the UV process to promote reactive radical species, including hydroxyl (HO'), chlorine (Cl'), and sulfate (SO₄-') radicals [11], [12], [14]. Previous work has shown that UV-AOPs inhibited algal cells but only partially reduced THMs and HANs formation [15]. Therefore, enhanced processes to effectively reduce THMs and HANs precursors are needed. Among the oxidants, UV with persulfate (UV/PS) appears to be the most readily applicable as it generates SO4-, which has higher selectivity than HO'. Compared with other persulfate activation methods (e.g., heat, transition metals, carbon), UV/PS is considered a cleaner process and

practical for drinking water treatment because it requires no heat, releases no additional chemicals, and does not increase sludge production [14]. Persulfate (PS) is also relatively cheap and has high stability during transportation [16]. Previous work has shown that UV/PS successfully reduced HANs formation potential of free amino acids and short oligopeptides [17]. In addition, the UV/PS was found to be more effective in reducing the formation of bromated HANs compared to UV/H₂O₂ [13].

As an alternative, the application of vacuum ultraviolet (VUV) light represents a promising approach to enhance UV-based advanced oxidation processes (UV-AOPs) for contaminant removal. A VUV lamp is a light source that emits wavelengths below 200 nm. A low-pressure mercury VUV lamp (hereafter referred to as VUV), encased in high-purity synthetic quartz glass (e.g., Suprasil quartz), emits two principal wavelengths at 185 and 254 nm. At 185 nm, water absorbs photons, leading to the formation of hydroxyl radicals (HO') via water photolysis, which drive contaminant degradation [16]. Notably, the energy consumption for 185 nm irradiation is comparable to that of 254 nm irradiation using the same light source, making the process more costeffective than conventional UV treatment [18]. VUV has been shown to remove various pollutants, including DOC [19], HANs [20], and DON [8], and its performance can be further enhanced by adding oxidants such as chlorine (Cl₂), ozone (O₃), or persulfate (PS) [8], [16], [18]. In particular, persulfate activation by VUV (VUV/PS) can generate both HO' and $SO_4^{-\bullet}$ (Equations (1)–(3)), with redox potentials of 2.8 V and 2.5–3.1 V, respectively, enabling synergistic oxidation.

$$H_2O + hv_{185} \rightarrow HO^{\bullet} + H^{\bullet}$$
 (1)

$$H_2O + hv_{185} \rightarrow HO^{\bullet} + H^{+} + e_{aq}^{-}$$
 (2)

$$S_2O_8^{2-} + hv_{185, 254} \rightarrow 2SO_4^{--}$$
 (3)

Despite these advantages, no studies have evaluated the VUV/PS process for treating algaeladen water, which contains complex mixtures of natural organic matter (NOM), dissolved organic nitrogen (DON), and disinfection byproduct (DBP) precursors. This gap is critical, as the presence of bromide in such waters can influence DBP speciation and toxicity, yet its effect under VUV/PS treatment remains unknown.



This study, for the first time, aimed to evaluate the potential of the VUV/PS process for treating coagulated and filtered real algae-laden water, with a focus on the removal of algal organic matter (AOM) as DBP precursors. Specifically, the objectives were to: 1) assess DOC and DON removal efficiency; 2) evaluate the DBP formation potential (DBPFP) and bromine incorporation factor (BIF) in treated water; and 3) characterize changes in AOM using fluorescence excitation-emission matrix (EEM) spectroscopy in relation to DBPFP. VUV and UV processes—alone and combined with varying PS concentrations—were systematically investigated. The findings provide insights into the efficacy of VUV/PS for mitigating AOM and DBP precursors in algae-laden waters.

2 Materials and Methods

2.1 Chemicals

Potassium persulfate (K₂S₂O₈; 97%; Ajax Finechem, Australia) was used as the oxidant in the UV/PS and VUV/PS processes. Sodium hypochlorite (NaOCl; 5%-6% w/w; commercial-grade; Haiter, Thailand) and ascorbic acid (99%; Carlo Erba, France) were used in the chlorination experiment. For the DBP analysis, monochloroacetonitrile (MCAN) (99%), trichloroacetonitrile (TCAN) (98%), and a mixed standard of THMs (CF (98%), DBCM (97%), BDCM (97%), and BF (99%)) (Sigma-Aldrich, USA) were used. Dichloroacetonitrile (98%) was purchased from Tokyo Chemical Industry, Japan, while DBAN (95%) and monobromoacetonitrile (MBAN) (98%) were obtained from Wako Pure Chemical Industries, Japan. All other chemicals and reagents (high performance liquid chromatograph or analytical grades) were acquired from local chemical suppliers.

2.2 Water sample preparation

The water sample was collected from the Sithan Lagoon at Khon Kaen University (KKU) in Thailand in April 2023. The Sithan Lagoon is a recreational waterbody on the KKU campus and experiences algal blooms. The water sample was pretreated by coagulation and sedimentation with polyaluminum chloride at 100 mg/L to remove colloidal particles. Following coagulation, the pH of the supernatant was adjusted to 7 using NaOH and HCl solutions. The water sample was then filtered using filter paper (no. 40;

pore size 8 μ m; Whatman, UK) and stored at 4 °C until use. DOC and UV₂₅₄ of coagulated/filtered water were 7.13 mg/L and 0.0728 cm⁻¹, respectively. More details of water characteristics are summarized in Table S1.

2.3 Experimental setup and procedure

Six duplicate experiments were conducted: 1) VUV, 2) VUV/PS (5 mg/L), 3) VUV/PS (50 mg/L), 4) UV, 5) UV/PS (5 mg/L), and 6) UV/PS (50 mg/L). The experiments were performed in 2 L batch cylinder reactors. Detailed information on the reactor setup and UV and VUV light sources is provided in the supplementary materials (Figure S1 and Text S1). The batch experiments investigated AOM removal by the VUV or UV irradiation processes compared to the PS activation processes. In the VUV/PS and UV/PS processes, K₂S₂O₈ solution was added to produce PS concentrations of 5 mg/L or 50 mg/L, representing low and high oxidant concentrations, respectively.

Each experiment lasted 60 min. During the reaction, the temperature was maintained at 25 ± 1 °C. The water was continuously mixed using a magnetic stirrer and recirculated using a peristaltic pump (300 mL/min). Water samples (100 mL) were collected at intervals of 0, 5, 10, 15, 30, and 60 min for DOC, DON, and UV absorbance at 254 nm (UV₂₅₄) analysis. The samples were filtered using a cellulose acetate membrane filter (0.45 μ m; Filtrex, India) and stored at 4 °C until analysis. The treated water (after 60 min) from each experiment was further analyzed for chlorinated DBPFP, and the AOM change was characterized by EEM.

2.4 DBP formation potential determination

The DBPFP of the chlorinated treated water was investigated. Water samples were buffered (pH 7; 10 mM phosphate buffer) and placed in a 40 mL amber glass vial for chlorination. The Cl_2 doses were determined from the DOC and NH_3 -N concentrations (Equation (4)) [8]. A stock Cl_2 solution was prepared from NaOCl solution. The water samples treated with Cl_2 were incubated in vials (no headspace) in dark conditions at 20 ± 1 °C for 24 h. The residual Cl_2 concentrations after 24 h were 4–6 mg/L. Following chlorination, the residual Cl_2 was quenched using ascorbic acid [8]. Only the water samples taken from the experiments at 0, 10, 30, and 60 min were analyzed for trihalomethanes formation potential (THMFP) and haloacetonitriles formation potential (HANFP).



$$Cl_2 \text{ dose } (mg/L) = [3 \times DOC (mg-C/L)] + [8 \times NH_3-N (mg-N/L)] + 10 (mg-Cl_2/L)$$
 (4)

2.5 Analytical methods

2.5.1 Characteristics of algae-laden water

The algae-laden water samples were characterized for DOC, DON, UV_{254} , specific UV absorbance (SUVA), EEM, chloride, and bromide ions. The DOC and total dissolved nitrogen (TDN) concentrations were determined using a total organic carbon/total nitrogen (TOC/TN) analyzer (multi N/C 2100S; Analytik Jena, Germany). The DON was determined by subtracting the dissolved inorganic nitrogen (NO₃-N, NO₂-N, and NH₃-N) concentrations from the TDN (Equation (5)). The methods used to analyze the NO₃-N, NO₂-N, and NH₃-N concentrations are described elsewhere [8].

DON
$$(mg/L) = TDN - NO_3 - N - NO_2 - N - NH_3 - N$$
 (5)

The UV_{254} was measured using a UV-visible spectrophotometer (DR6000; Hack, USA). The EEM was analyzed using a spectrofluorometer (FS5; Edinburgh Instruments, United Kingdom) following the setting and correction procedure described by Ranthom [21]. An ion chromatograph (940 Professional IC Vario; Metrohm, Switzerland) was used to analyze the chloride and bromide ions in the water samples.

2.5.1 Determination of THMFP and HANFP

The THMFP and HANFP concentrations in the chlorinated samples were extracted using a liquid–liquid extraction method. Steps of the extraction procedure are described in Supplementary material (Text S2). A gas chromatograph (GC) with an electron capture detector (GC-ECD) (Nexis GC-2030; Shimadzu, Japan) was used to analyze the THMs and HANs concentrations. Detail of the GC condition is also described in the supplementary materials (Text S2).

3 Results and Discussion

3.1 Reduction of DOC, UV₂₅₄, and DON by VUV and UV processes

Figure 1 shows DOC and DON removal and UV₂₅₄ reduction by the VUV and UV processes with and without the inclusion of PS. In the VUV process, the

DOC concentrations decreased progressively with both increasing PS dosage and extended reaction times. In contrast, the UV process showed minimal to negligible impact on DOC concentrations, regardless of treatment conditions. Table 1 shows the DOC removal rates and removal efficiencies by the VUV and UV processes. The relationship between $\ln (C/C_0)$ and time in the VUV process was linear, indicating a first-order kinetic reaction with a removal rate constant (k) value of $0.0052-0.0083 \text{ min}^{-1}$. The VUV process removed 30%-40% of the DOC at 60 min, with the highest removal at a PS dose of 50 mg/L (Figure 1a). In the UV process, only the UV/PS (PS at 50 mg/L) process fit the first-order kinetic reaction, with a k value of 0.0030 min^{-1} (R² = 0.8919), while the DOC removal efficiency was approximately 14% at 60 min (Figure 1(d) and Table 1).

The results showed that UV₂₅₄ reduction followed the first-order kinetic reaction in the VUV/PS and UV/PS processes at PS doses of 5 and 50 mg/L, as well as the processes without PS. The initial k values (15 min) and removal efficiencies (60 min) of UV₂₅₄ are shown in Table 1. In both the VUV and UV processes, UV₂₅₄ gradually decreased with increasing reaction time and PS doses. The k values and reduction efficiencies for UV254 under the VUV processes were 0.0609–0.0939 min⁻¹ and 72%–78%, respectively (Figure 1(b) and Table 1). In the UV/PS process, the k values and reduction efficiencies of UV_{254} were 0.0266–0.0876 min⁻¹ and 57%–82%, respectively (Figure 1(e) and Table 1). Overall, the VUV and UV processes with and without the inclusion of PS decreased the SUVA values by 54%-78% (Table S2).

Increasing the PS concentration to 50 mg/L in the UV and VUV processes increased the DOC removal rates by 15.0 and 41.5 times, respectively, and increased the UV₂₅₄ reduction rate by 3.3 and 3.5 times, respectively, compared with the UV alone. The DOC removal rate was higher in the VUV/PS process than the UV/PS process, which was due to the production of more reactive radical species (SO₄- and HO·) (Equations (1)–(3)) in the VUV/PS process. In addition, HO· (water homolysis at 185 nm) reacted with the PS to produce more SO₄- (Equation (6)), and SO₄- reacted with water to form more HO· (Equation (7)) [12], [16].

$$\text{HO}^{\bullet} + \text{S}_2\text{O}_8^{2-} \rightarrow 0.5\text{O}_2 + \text{SO}_4^{-\bullet} + \text{HSO}_4^{-}$$
 (6)
 $\text{SO}_4^{-\bullet} + \text{H}_2\text{O} \rightarrow \text{SO}_4^{2-} + \text{HO}^{\bullet} + \text{H}^{+}$ (all pH)

$$k = 5.0 \times 10^2 \,\mathrm{M}^{-1} \mathrm{s}^{-1} \tag{7}$$



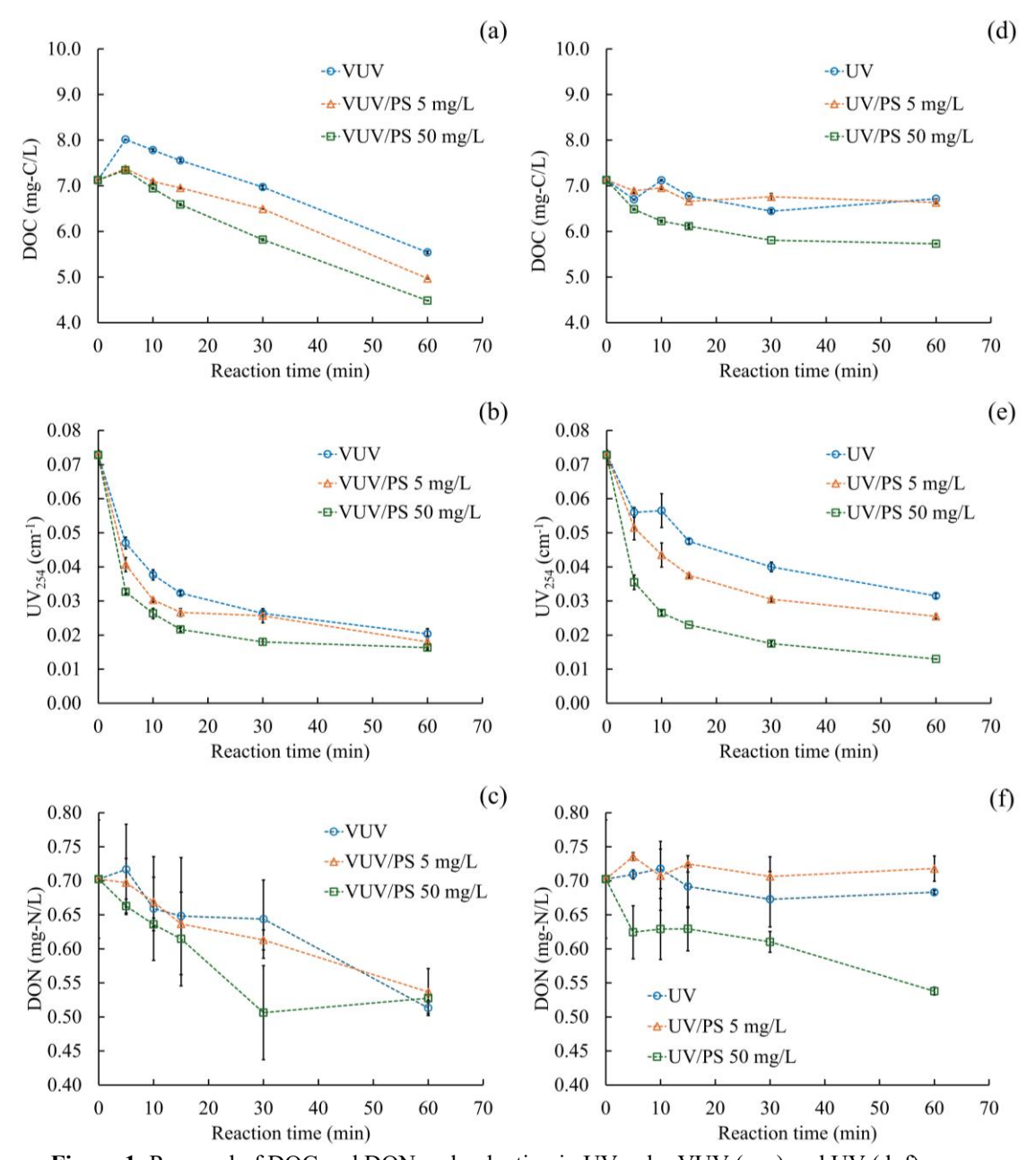


Figure 1: Removal of DOC and DON and reduction in UV₂₅₄ by VUV (a-c) and UV (d-f) processes.

Increasing the PS dose to 50 mg/L in the VUV process improved the DOC removal and UV $_{254}$ reduction rates by 60% and 54%, respectively, compared with the VUV alone. These results correspond with previous research that reported an increase in the natural organic matter (TOC = 3.83 mg/L) removal rate of 81% using a VUV/peroxymonosulphate process compared with VUV-only [22].

Removal of DON by the VUV, VUV/PS (5 and 50 mg/L), and UV/PS processes varied slightly between 24% and 27% at 60 min (or UV $_{254}$ fluence of 15,840 mJ/cm²) (Figure 1(c) and (f)). The rapid reductions observed in the VUV/PS (50 mg/L) process during the first 30 min may have been due to sulfate radicals produced by the high PS dose of PS.



Рисседор	DOC a			UV_{254}^{b}		
Processes	$k_{\rm obs}~({\rm min}^{-1})$	\mathbb{R}^2	Removal (%)	$k_{\rm obs}~({\rm min}^{-1})$	\mathbb{R}^2	Reduction (%)
VUV	0.0052	0.94	29.52	0.0609	0.98	72.08
VUV/PS (5 mg/L)	0.0069	0.99	34.61	0.0767	0.97	75.29
VUV/PS (50 mg/L)	0.0083	0.99	39.79	0.0939	0.95	77.57
UV	0.0002	0.02	0.00	0.0266	0.96	56.75
UV/PS (5 mg/L)	0.0004	0.21	0.52	0.0490	0.98	64.99
UV/PS (50 mg/L)	0.0030	0.89	13.57	0.0876	0.96	82.15

Notes: a DOC removal rate, R², and efficiency were assessed at 60 min; b Initial UV₂₅₄ reduction rate and R² at 15 min, and UV₂₅₄ efficiency at 60 min.

In contrast, steady DON removals were seen in the VUV and VUV/PS (5 mg/L) processes. In the VUV and VUV/PS processes, DON removals were less than DOC removals. Similar trends have been reported for DOC and DON in surface waters treated with VUV (24 J/cm²) [8] and UV/PS processes [13]. This low DON removal efficiency is likely because DON accounts for approximately 10% of DOC and nitrogen is bound to the center of various organic compounds, including humic acid, fulvic acid, amino acids (both free and combined forms), nucleic acids, and a range of unidentified substances [13], [23]. Moreover, strong nitrogen-containing bonds, such as triazine rings and C–N single bonds, have been reported to resist mineralization by VUV/H₂O₂ [24].

3.2 Characterization of AOM in coagulated and AOP-treated algae-laden water using EEM

The AOM composition of the coagulated/filtered and treated algae-laden water samples was characterized. Figure 2 presents the 3D-EEM contours of the coagulated/filtered and treated algae-laden water for the VUV and UV processes with and without PS. Four groups of natural organic matter were classified based on major fluorescence peaks, including terrestrial fulvic-like (peak A; EX/EM 250/400 nm), terrestrial humic-like (peak C; EX/EM 350/450 nm), tryptophan protein-like (peak T; EX/EM 275/340 nm), and tyrosine protein-like (peak B; EX/EM 275/300 nm) [21], [25].

The coagulated/filtered algae-laden water (Figure 2(a)) contained two major components (peaks A and C). Peak picking analysis (Figure 3 and Table S3) showed that fulvic-like and humic-like dissolved organic matter (DOM) (71% of the total fluorescence intensities) were the main components in the coagulated/filtered algae-laden water, which was consistent with the results for an algae-laden surface water sample in a previous study [10]. The source of fulvic-like and humic-like substances could be surface runoff carrying decayed vegetation. However, as the fluorescence index (FI) of

the coagulated algae-laden water was 2.1 (> 1.9) (Table S3), it is likely that the fulvic acid was microbially derived DOM [26]. Therefore, the DOM from this surface water source could mainly comprise of AOM.

Overall, the VUV and UV-AOPs successfully reduced all AOM groups (Figure 2). Substantial decreases in fulvic-like and humic-like substances were observed in the VUV and UV processes (Figure 3). The VUV processes with and without PS reduced fulvic-like AOM (94%–97%) and humic-like AOM (94%–96%). In comparison, the UV process with high PS (50 mg/L) decreased fulvic-like and humic-like AOMs by up to 95%, while the UV processes without PS or with low PS (5 mg/L) achieved smaller reductions in fulvic-like and humic-like AOMs of 41%–62%. This could be due to direct photolysis at 185 nm and/or higher SO₄-* and HO* breaking down organic structures more intensively than under UV photolysis (254 nm) or UV/PS (low dose) [8], [27], [28].

Furthermore, smaller reductions in peaks T and B were observed in the UV process compared to the fulvic-like and humic-like compounds. This may have been because peaks T and B contained less aromatic and unsaturated carbon, making them less reactive to UV photolysis.

These results suggest that radicals (SO₄- and HO')—particularly in the VUV/PS process preferentially broke the unsaturated structures of the fulvic-like and humic-like DOMs compared to protein-like compounds [27], [28]. Given that the fulvic-like and humic-like DOMs promoted C-DBPs [28], [29] and the protein-like DOMs produced N-DBPs [29], the VUV processes have the potential to treat water sources containing AOM. It should be noted that the results of this study are based on real algae-laden water, rather than solely on organic compounds that react with radicals. The presence of inorganic ions such as Cl-, CO32-, and NO3- can scavenge reactive radicals [12], [30], thereby reducing process efficiency. This effect should be taken into account when applying VUV/PS treatment.



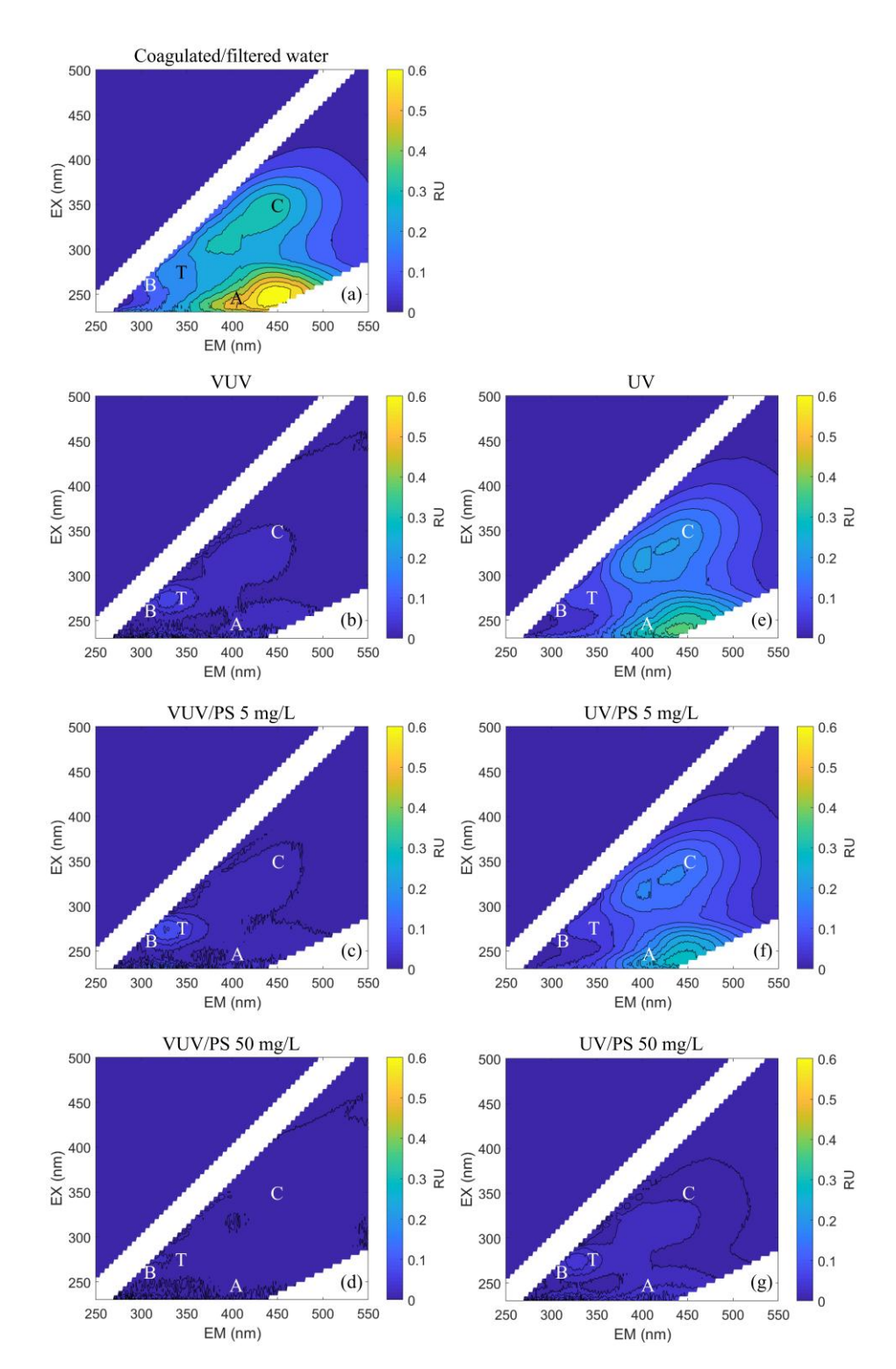


Figure 2: EEM spectra of coagulated/filtered and treated algae-laden water (a) from VUV (b–d) and UV (e)–(g) processes.



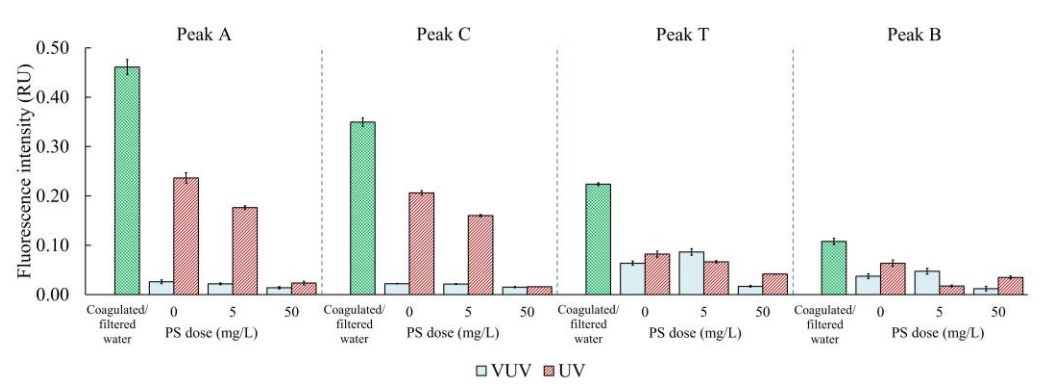


Figure 3: Fluorescence intensities at peaks A, C, T, and B from coagulated/filtered and treated algae-laden water from VUV and UV processes.

3.3 Determination of DBPFP in VUV and UV-based processes

Figures 4 and 5 show the THMFP and HANFP concentrations and BIFs in the water samples treated with the VUV and UV processes with and without PS, respectively (Tables S4 and S5). The water samples in the VUV and UV processes taken at 0, 10, 30, and 60 min were used to determine the DBPFP and calculation of the BIF (Equations (8) and (9)) [31].

$$BIF - THMs = \frac{(0 \times [CF]) + (1 \times [BDCM]) + (2 \times [DBCM]) + (3 \times [BF])}{[CF] + [BDCM] + [DBCM] + [BF]}$$
(8)

$$BIF - HANs = \frac{(0 \times [MCAN]) + (0 \times [DCAN]) + (1 \times [MBAN]) + (2 \times [DBAN])}{[MCAN] + [DCAN] + [MBAN] + [DBAN]}$$
(9)

where the THM and HAN concentrations are on a molar basis. The degree of substitution by bromine in THMs, the BIF values range from 0 (no brominated THM) to 3 (brominated THM). The BIF values range from 0 (no brominated HAN) to 2 (brominated HAN) for HANs. Four THMs and five HANs were analyzed following chlorination for 24 h. Figure 4 shows that CF was the predominant THM species detected, with concentrations ranging between 127 µg/L and 246 µg/L. The BDCM, DBCM, and BF concentrations were 31.6-46.9 µg/L, 6.2–8.6 μg/L, and 0.1–0.3 μg/L, respectively. Increasing the reaction time and PS dose in the VUV process gradually decreased THMFP by 39%-43% (Figure 4(a)-(c)). In the UV process, THMFP was reduced by 8%-27% (Figure 4(d)–(f)), which was approximately 1.4 times less than in the VUV process.

Figure 5 shows the concentrations of HAN species, with DCAN the major compound detected

(2.45–3.82 μ g/L). Formation of MBAN (0.21–0.40 μ g/L), MCAN (0.13–0.30 μ g/L), TCAN (0.09–0.29 μ g/L), and DBAN (0.02–0.10 μ g/L) was much lower than DCAN. The VUV and UV processes with and without PS decreased HANPF by 10%–22%.

While CF and DCAN were the major THMs and HANs species, brominated THMs and HANs were also formed. This could be due to bromide ions (114 μ g/L) in the source water. Table S6 shows the ratios of the THMs to their respective WHO guideline values. The sum of each ratio ranged between 1.05 and 1.61, which was higher than the WHO guideline values (1.00).

However, the VUV processes with and without PS (at 60 min) produced ratio sums (1.05–1.09) close to the WHO guideline values, while the UV processes with and without PS (5 and 50 mg/L) produced only small changes and the ratios remained close to the initial THMs ratio. As such, further treatment would be required to reduce the sum of the THMs ratio below the WHO guideline level.

The DOC and EEM reductions followed a similar trend to the THMFP reduction. For example, the VUV processes with and without PS reduced peak A (fluvic-like) by 94%–97% and peak C (humic-like) by 94%-96% and decreased CF by 43%-48%. In the UV processes with and without PS, peaks A and C reduced by 49%-95% and 41%-95%, respectively, and CF decreased by 9%-29% while less reduction was observed for both protein-likes (peak B and T) and HANFP. These results indicate that the VUV and VUV/PS processes were more effective at removing THM precursors than those of HANs. Regarding HANFP, the DCAN and DBAN concentrations were below than the WHO guideline values. The VUV process, with and without PS, achieved a substantial reduction in DBANFP, while DCANFP remained comparable to that of UV-AOPs (Table S5).

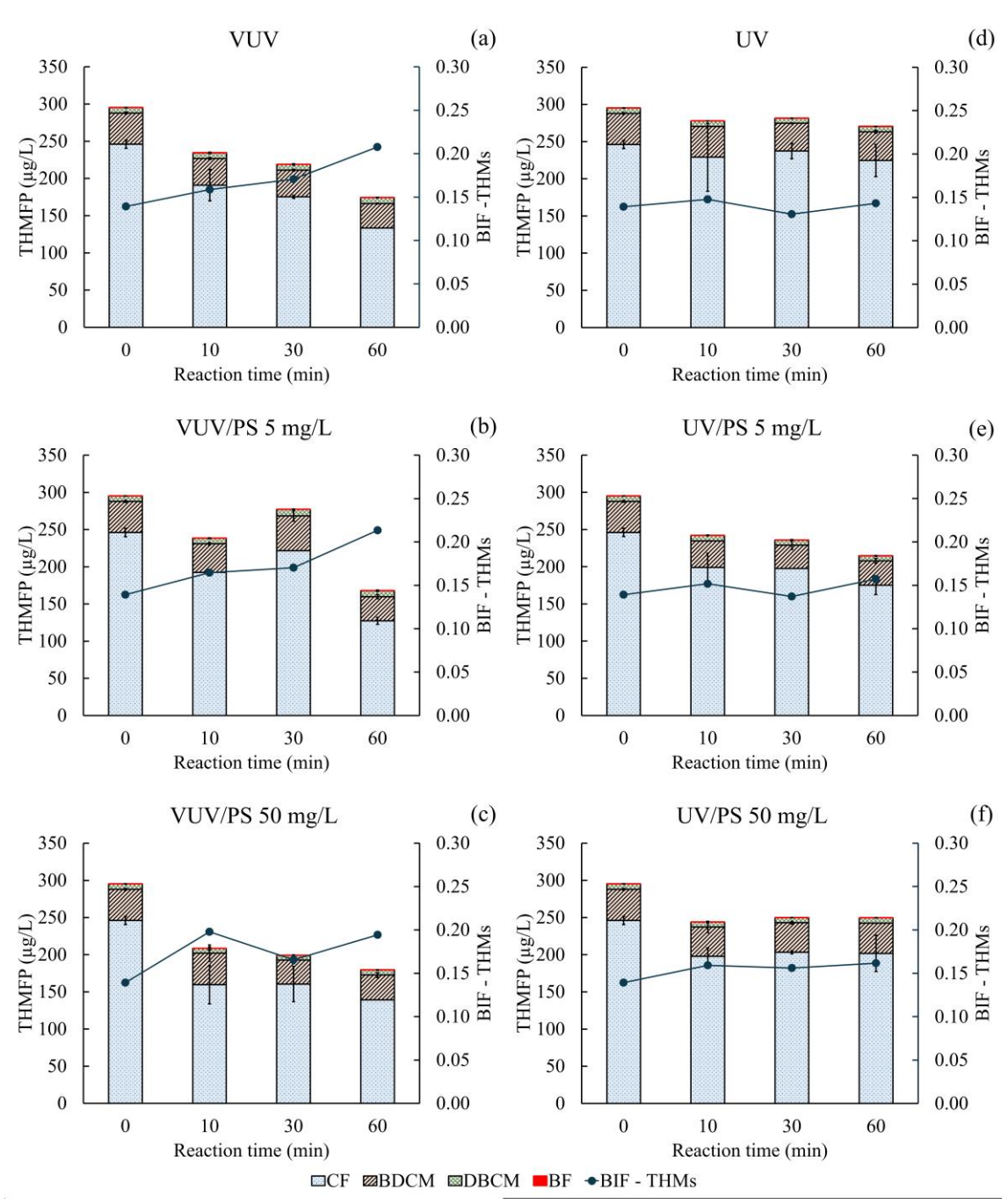


Figure 4: THMFP of chlorinated treated water and BIF from VUV (a-c) and UV (d-f) processes.



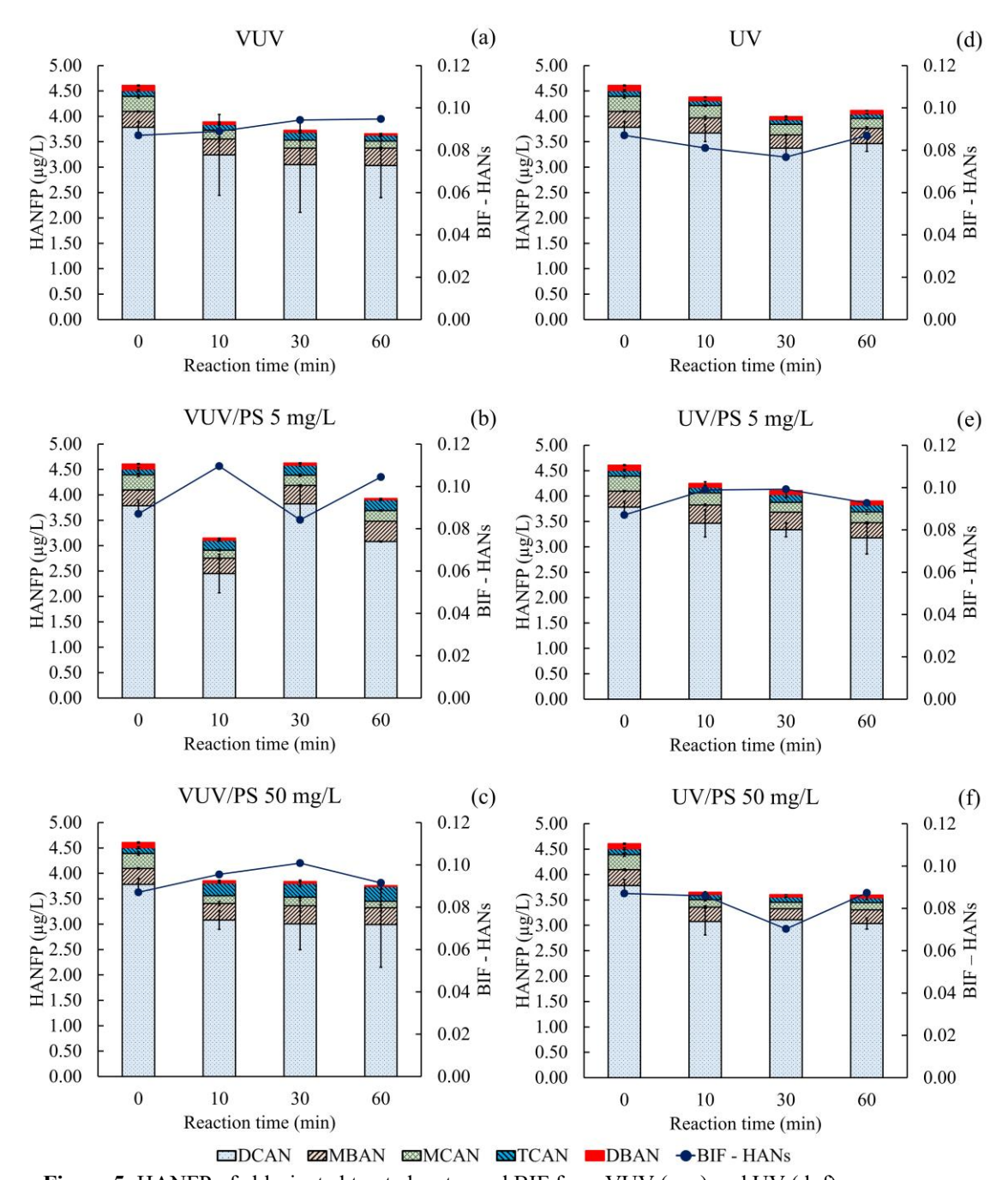


Figure 5: HANFP of chlorinated treated water and BIF from VUV (a-c) and UV (d-f) processes.

Additionally, BIF was used to determine how bromine atom is incorporated in DBP formation upon reaction with chlorine, ultimately affecting the toxicity of these compounds since brominated DBPs are more toxic than chlorinated DBPs [31]. It is noted that TCAN was not used to calculate BIF because of the

instability of the compound, which is easy to be hydrolyzed [24].

For THMFP, the THM-BIF increased with reaction time during VUV-AOPs but remained stable following UV-AOPs. The increase in BIF (VUV-AOPs; Figure 4(a)–(c) indicates that the proportion of



chlorinated THMs (CF) decreased more substantially than that of brominated THMs. In the case of HANFP, the HAN-BIF values fluctuated or remained relatively constant for both VUV-AOPs and UV-AOPs. These results suggest a similar reduction in the proportions of chlorinated and brominated HANFPs by VUV-AOPs and UV-AOPs. VUV and VUV/PS effectively reduced THMFP and HANFP. Although the sum of THM ratios slightly exceeded the WHO guideline, further optimization of operating conditions may ensure compliance with regulatory standards.

4 Conclusions

This study compared VUV/PS, VUV, UV/PS, and UV processes for DOC, UV₂₅₄, and DON removals from algae-laden water. The VUV/PS (50 mg/L) process performed best at removing DOC (40% in 60 min), UV₂₅₄, and DON. All fluorophore groups were effectively removed by the VUV/PS (5 and 50 mg/L), VUV, and UV/PS (50 mg/L) processes. Chloroform and DCAN were the highest THMFP and HANFP species, respectively. The reductions in DOC and EEM peaks corresponded with THMFP reductions. The VUV and VUV/PS processes produced the highest THMFP reductions (~40%). Brominated THMFP decreased after VUV and VUV/PS processes, except for only slight increase of DBCM and BF. No differences in HANFP were found for the VUV and UV processes with and without PS. Overall, the VUV and VUV/PS processes demonstrated potential as a pretreatment to reduce DBPFP in algae laden water. Future work should focus on evaluating these processes under continuous-flow pilot-scale conditions, assessing energy efficiency, examining their performance across different water matrices and seasonal variations. Additionally, integrating VUV-based AOPs with downstream biological filter treatment could further enhance DBP precursor removal and overall process sustainability.

Acknowledgments

This study received the following funding: 1) National Research Council of Thailand (NRCT) (Contact No. N41A660161), 2) Research and Graduate Studies Fund for Supporting Lecturers to Admit High Potential Students to Study and Research on His Expert Program, Graduate School, Khon Kaen University, 3) Kurita Water and Environment Foundation (22Pth015-I4), 4) Research Program funding from

Research Innovation Department Khon Kaen University, and 5) Fundamental fund 2025–2026.

Author Contributions

S.S.: Methodology, validation, formal analysis, investigation, visualization, and writing (original draft); P.K.: Methodology and formal analysis; P.J.: Methodology, investigation, formal analysis, and writing (review and editing); S.S.R.: Writing (review and editing) and supervision; E.K.: Writing (review and editing) and supervision; T.R.: Conceptualization, methodology, validation, funding acquisition, project administration, supervision, and writing (review and editing). All authors have read and agreed to the published version of the manuscript.

Conflicts of Interest

The authors declare no conflict of interest.

References

- [1] R. Connor, The United Nations World Water Development Report 2024: water for prosperity and peace; executive summary, UNESCO World Water Assessment Programme. France: UNESCO, Mar. 2024.
- [2] T. Somdee, T. Kaewsan, and A. Somdee, "Monitoring toxic cyanobacteria and cyanotoxins (microcystins and cylindrospermopsins) in four recreational reservoirs (Khon Kaen, Thailand)," *Environmental Monitoring and Assessment*, vol. 185, pp. 9521–9529, 2013, doi: 10.1007/s10661-013-3270-8.
- [3] M. Schneider and L. Bláha, "Advanced oxidation processes for the removal of cyanobacterial toxins from drinking water," *Environmental Sciences Europe*, vol. 32, pp. 1–15, 2020, doi: 10.1186/s12302-020-00371-0.
- [4] F. Dong, Q. Lin, C. Li, G. He, and Y. Deng, "Impacts of pre-oxidation on the formation of disinfection byproducts from algal organic matter in subsequent chlor(am)ination: A review," *Science of the Total Environment*, vol. 754, pp. 1–15, 2021, doi: 10.1016/j.scitotenv. 2020.141955.
- [5] X. Li, N. R. H. Rao, K. L. Linge, C. A. Joll, S. Khan, and R. K. Henderson, "Formation of algalderived nitrogenous disinfection by-products during chlorination and chloramination," *Water*



- Research, vol. 183, pp. 1–10, 2020, doi: 10.1016/j.watres.2020.116047.
- [6] Y. Chen et al., "UV-assisted chlorination of algae-laden water: Cell lysis and disinfection byproducts formation," *Chemical Engineering Journal*, vol. 383, 2020, Art. no. 123165, doi: 10.1016/j.cej.2019.123165.
- [7] K. Foreman et al., "Effects of harmful algal blooms on regulated disinfection byproducts: Findings from five utility case studies," *AWWA Water Science*, vol. 3, pp. 1–21, 2021, doi: 10.1002/aws2.1223.
- [8] P. Kiattisaksiri, E. Khan, P. Punyapalakul, C. Musikavong, D. C. W. Tsang, and T. Ratpukdi, "Vacuum ultraviolet irradiation for mitigating dissolved organic nitrogen and formation of haloacetonitriles," *Environmental Research*, vol. 185, 2020, Art. no. 109454, doi: 10.1016/j.envres.2020.109454.
- [9] Y. Zhang, W. Chu, D. Yao, and D. Yin, "Control of aliphatic halogenated DBP precursors with multiple drinking water treatment processes: Formation potential and integrated toxicity," *Journal of Environmental Sciences*, vol. 58, pp. 322–330, 2017, doi: 10.1016/j.jes.2017.03.028.
- [10] J. Ma et al., "Enhanced coagulation of covalent composite coagulant with potassium permanganate oxidation for algae laden water treatment: Algae and extracellular organic matter removal," *Chemical Engineering Journal Advances*, vol. 13, Art. no. 100427, 2023, doi: 10.1016/j.ceja. 2022.100427.
- [11] X. Lei, Y. Lei, X. Zhang, and X. Yang, "Treating disinfection byproducts with UV or solar irradiation and in UV advanced oxidation processes: A review," *Journal of Hazardous Materials*, vol. 408, 2021, Art. no. 124435, doi: 10.1016/j.jhazmat.2020.124435.
- [12] Y. L. Zhang et al., "Promotive effects of vacuum-UV/UV (185/254 nm) light on elimination of recalcitrant trace organic contaminants by UV-AOPs during wastewater treatment and reclamation: A review," *Science of the Total Environment*, vol. 818, 2022, Art. no. 151776, doi: 10.1016/j.scitotenv.2021.151776.
- [13] Y. Murata, H. Sakai, and K. Kosaka, "Degrading surface-water-based natural organic matter and mitigating haloacetonitrile formation during chlorination: Comparison of UV/persulfate and UV/hydrogen peroxide pre-treatments," Chemosphere,

- vol. 354, 2024, Art. no. 141717, doi: 10.1016/j.chemosphere.2024.141717.
- [14] F. Zhang and M. Sui, "Progress of persulfate-based advanced oxidation process (PS-AOPs) coupled with ultrafiltration membrane to alleviate membrane fouling: A review," Environmental Engineering Research, vol. 30, 2024, Art. no. 240244, doi: 10.4491/eer.2024.244.
- [15] F. Dong, Q. Lin, J. Deng, T. Zhang, C. Li, and X. Zai, "Impact of UV irradiation on Chlorella sp. damage and disinfection byproducts formation during subsequent chlorination of algal organic matter," *Science of the Total Environment*, vol. 671, pp. 519–527, 2019, doi: 10.1016/j.scitotenv.2019.03.282.
- [16] D. Wen, W. Li, J. Lv, Z. Qiang, and M. Li, "Methylene blue degradation by the VUV/UV/persulfate process: Effect of pH on the roles of photolysis and oxidation," *Journal of Hazardous Materials*, vol. 391, 2020, Art. no. 121855, doi: 10.1016/j.jhazmat.2019.121855.
- [17] W. Chu, D. Li, Y. Deng, N. Gao, Y. Zhang, and Y. Zhu, "Effects of UV/PS and UV/H₂O₂ pre-oxidations on the formation of trihalomethanes and haloacetonitriles during chlorination and chloramination of free amino acids and short oligopeptides," *Chemical Engineering Journal*, vol. 301, pp. 65–72, 2016, doi: 10.1016/j.cej. 2016.04.003.
- [18] H. Zhang, W. Sun, J. Zhang, and J. Ma, "Vacuum-ultraviolet based advanced oxidation and reduction processes for water treatment," *Journal of Hazardous Materials*, vol. 471, 2024, Art. no. 134432, doi: 10.1016/j.jhazmat.2024. 134432.
- [19] P. Kiattisaksiri, N. Petmark, and T. Ratpukdi, "Combination of coagulation and VUV+H₂O₂ for the treatment of color and organic matter in treated effluent wastewater from a sugar factory," *Applied Science and Engineering Progress*, vol. 16, no. 4, p. 6192, 2023, doi: 10.14416/j.asep.2022.08.002.
- [20] P. Kiattisaksiri, E. Khan, P. Punyapalakul, and T. Ratpukdi, "Photodegradation of haloacetonitriles in water by vacuum ultraviolet irradiation: Mechanisms and intermediate formation," *Water Research*, vol. 98, pp. 160–167, 2016, doi: 10.1016/j.watres.2016.04.010.
- [21] N. Ranthom, W. Khongnakorn, and P. Jutaporn, "MIEX resin and enhanced coagulation treatment of high-bromide natural water: Chlorine reactivity



- and DBP precursors removal," *Journal of Environmental Chemical Engineering*, vol. 11, 2023, Art. no. 111497, doi: 10.1016/j.jece.2023. 111497.
- [22] Z. Amiri, G. Moussavi, S. Mohammadi, and S. Giannakis, "Development of a VUV-UVC/ peroxymonosulfate, continuous-flow advanced oxidation process for surface water disinfection and natural organic matter elimination: Application and mechanistic aspects," *Journal of Hazardous Materials*, vol. 408, 2021, Art. no. 124634, doi: 10.1016/j.jhazmat.2020.124634.
- [23] H. W. Chen, C. Y. Chen, and G. S. Wang, "Performance evaluation of the UV/H₂O₂ process on selected nitrogenous organic compounds: Reductions of organic contents vs. corresponding C-, N-DBPs formations," *Chemosphere*, vol. 85, no. 4, pp. 591–597, 2011.
- [24] B. Li, F. Yang, B. Chen, J. Li, L. Zhu, and W. T. Li, "Detecting trace dissolved organic nitrogen (DON) in freshwater by converting DON rapidly into nitrate with VUV/H₂O₂ pretreatment," *Chemosphere*, vol. 307, 2022, Art. no. 135790, doi: 10.1016/j.chemosphere.2022.135790.
- [25] P. G. Coble, "Characterization of marine and terrestrial DOM in seawater using excitation-emission matrix spectroscopy," *Marine Chemistry*, vol. 51, pp. 325–346, 1996, doi: 10.1016/0304-4203(95)00062-3.
- [26] M. P. Miller, D. M. McKnight, and S. C. Chapra, "Production of microbially-derived fulvic acid from photolysis of quinone-containing extracellular

- products of phytoplankton," *Aquatic Sciences*, vol. 71, pp. 170–178, 2009, doi: 10.1007/s00027-009-9194-2.
- [27] G. Ji et al., "Study on the removal of humic acid by ultraviolet/persulfate advanced oxidation technology," *Environmental Science and Pollution Research*, vol. 27, pp. 26079–26090, 2020, doi: 10.1007/s11356-020-08894-y.
- [28] X. Li et al., "Molecular transformation of dissolved organic matter during persulfate-based advanced oxidation: Response of reaction pathways to structure," *Chemical Engineering Journal*, vol. 474, 2023, Art. no. 146256, doi: 10.1016/j.cej.2023.146256.
- [29] P. Jutaporn, M. D. Armstrong, and O. Coronell, "Assessment of C-DBP and N-DBP formation potential and its reduction by MIEX® DOC and MIEX® GOLD resins using fluorescence spectroscopy and parallel factor analysis," *Water Research*, vol. 172, 2020, Art. no. 115460, doi: 10.1016/j.watres.2019.115460.
- [30] R. J. P. Latiza, R. V. Rubi, and A. Quitain, "Supercritical water gasification for hospital wastewater," *Journal of Hazardous Materials Advances*, 2025, Art. no. 100651, doi: 10.1016/ j.hazadv.2025.100651.
- [31] M. Usman, M. Hüben, T. Kato, C. Zwiener, T. Wintgens, and V. Linnemann, "Occurrence of brominated disinfection by-products in thermal spas," *Science of the Total Environment*, vol. 845, 2022, Art. no. 157338, doi: 10.1016/j.scitotenv.2022.157338.



Supplementary Material

Text S1: Reactor setup and light source information

The reactor setup is shown in Figure S1. A glass cylindrical reactor (diameter 8.0 cm and height 45.5 cm) with an aluminum foil cover was used. The light source (VUV or UV) was positioned at the center of the reactor. The reactor temperature was maintained at 25 ± 1 °C using a water jacket. A magnetic stirrer was employed to mix the algal-laden water, and a peristaltic pump recirculated the water.

Each reactor was equipped with two VUV (185+254 nm, model GPH383T5/VH/HO, Universal Lights Source, Inc., USA) or UV (254 nm, model GPH383T5/L/HO, Universal Lights Source, Inc., USA) lamps. The average effective path length of UV photons at a wavelength of 254 nm was calculated to be approximately 6.85 cm by fitting the kinetics of lowconcentration H₂O₂ degradation with UV [2]. The photon flux of the UV lamp entering the water was determined by the iodide/iodate actinometer [1]. The VUV photon flux at a wavelength of 185 nm was determined by the H₂O₂ production rate from VUV radiation into the water [2]. The calculated photon intensity of VUV and UV entering the water were approximately 1.28 and 10.67 μeinstein/s, corresponding to fluence rate of 0.73 mW/cm² and 4.40 mW/cm², respectively.

Text S2: THMFP and HANFP extraction and analysis

The THMFP and HANFP concentrations in the chlorinated samples were extracted using a liquid–liquid extraction method. (US EPA Method 551.1) [3]. A water sample of 25 mL was added to a 40 mL clear glass vial. The sample was adjusted to pH 4.5–5.5 using 2 N H₂SO₄. Next, 5 g of Na₂SO₄ was added to

the adjusted sample to increase the ionic strength. Following this, 2.5 mL of methyl tert-butyl ether (MTBE) was added and the vial was sealed with a polypropylene screw cap with Telfon® faced septum. The vial was vigorously shaken for 2 min and allowed to stand for 4 min. The MTBE layer (extracted sample) was collected in a 2 mL amber vial and stored in a freezer (below -10 °C) until analysis (within 7 d).

A gas chromatograph (GC) with an electron capture detector (GC-ECD) (Nexis GC-2030; Shimadzu, Japan) was used to analyze the THMs and HANs concentrations using an injection volume of 1 μL of the extracted sample. The GC was fitted with a Rtx[®]-5 fused silica capillary column (30 m \times 0.25 mm I.D. × 0.25 μm film thickness; Restek, USA). Helium (mL/min) and nitrogen (15 mL/min) were used as the carrier and makeup gases. The injection port and detector temperatures were set at 250 °C. The GC temperature program began at 35 °C for 5 min, after which it increased to 240 °C (40 °C/min) for 1 min. The retention times were CF (2.8 min), BDCM (4.3 min), DBCM (6.2 min), BF (7.2 min), TCAN (3.7 min), MCAN (3.8 min), DCAN (4.7 min), DBAN (6.0 min), and MBAN (7.5 min). The THMs and HANs detection limits were 0.1 and 0.01 µg/L, respectively.

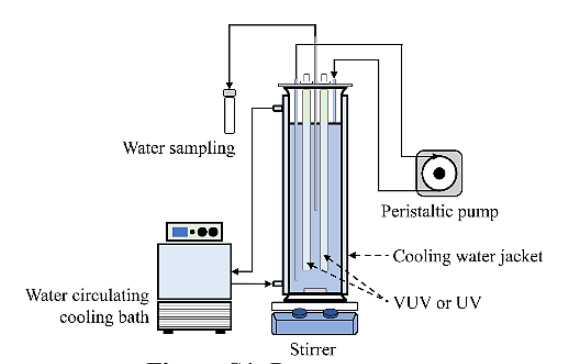


Figure S1: Reactor setup.

Table S1: Characteristics of raw and coagulated/filtered algae-laden water.

Parameter	Unit	Raw Water	Coagulated/Filtered Algae-Laden Water
pН	-	6.61	7.06 ± 0.01
Turbidity	NTU	96.5	1.28 ± 0.02
UV_{254}	cm^{-1}	-	0.0728 ± 0.0013
DOC	mg-C/L	24.11 ± 0.0026	7.13 ± 0.57
SUVA	L/mg-C · m	-	1.03 ± 0.07
TDN	mg-N/L	6.84 ± 0.08	1.05 ± 0.08
NO ₃ -N	mg-N/L	-	0.0205 ± 0.0055
NO ₂ -N	mg-N/L	-	0.0020 ± 0.0005
NH ₃ -N	mg-N/L	-	0.3206 ± 0.0474
DON	mg-N/L	-	0.70 ± 0.09
Chloride	mg/L	-	295.55
Bromide	mg/L	-	0.114 ± 0.062

Notes: values are averages \pm standard deviations



Table S2: SUVA values of treated water under VUV and UV systems.

Processes				SUVA (L/mg-C	· m) at	React	ion Time	2		
riocesses	5 min		1	l0 min	15 min			3	0 min	60 min	
VUV	0.5867	± 0.0188	0.4844	± 0.0105	0.4284	± 0.	0190	0.3787	± 0.0183	0.3670	± 0.0067
VUV/PS 5 mg/L	0.5517	\pm 0.0351	0.4279	\pm 0.0154	0.3835	\pm 0.	0168	0.3949	\pm 0.0235	0.3421	± 0.0010
VUV/PS 50 mg/L	0.4458	\pm 0.0294	0.3808	\pm 0.0433	0.3291	\pm 0.	0172	0.3107	± 0.0351	0.3656	± 0.0340
UV	0.8358	\pm 0.0141	0.7932	± 0.0601	0.7012	\pm 0.	0156	0.6206	\pm 0.0022	0.4691	± 0.0110
UV/PS 5 mg/L	0.7495	\pm 0.0867	0.6266	± 0.0706	0.5631	\pm 0.	0130	0.4529	\pm 0.0446	0.3846	± 0.0209
UV/PS 50 mg/L	0.5472	± 0.0214	0.4257	\pm 0.0060	0.3761	\pm 0.	0022	0.3014	± 0.0015	0.2270	± 0.0067

Table S3: Fluorescence intensity and fluorescence index of coagulated/filtered and treated water under VUV and UV systems.

D		Fluorescence Intensity (RU)											El Il		
Processes	I	eak A	4	l	Peak (С	Peak T		Peak B			Fluorescence Index			
Coagulated water	0.461	±	0.015	0.350	±	0.009	0.224	±	0.003	0.108	±	0.006	2.103	±	0.022
VUV	0.026	\pm	0.004	0.022	\pm	0.000	0.064	\pm	0.004	0.037	\pm	0.005	1.562	\pm	0.037
VUV/PS 5 mg/L	0.022	\pm	0.002	0.022	\pm	0.001	0.086	\pm	0.007	0.047	\pm	0.006	1.547	\pm	0.069
VUV/PS 50 mg/L	0.014	\pm	0.002	0.015	\pm	0.001	0.017	\pm	0.002	0.012	\pm	0.005	1.559	\pm	0.047
UV	0.236	\pm	0.011	0.206	\pm	0.005	0.082	\pm	0.006	0.064	\pm	0.007	1.945	\pm	0.029
UV/PS 5 mg/L	0.176	\pm	0.004	0.160	\pm	0.002	0.066	\pm	0.002	0.017	\pm	0.002	2.001	\pm	0.036
UV/PS 50 mg/L	0.024	\pm	0.004	0.016	\pm	0.000	0.042	\pm	0.000	0.035	\pm	0.003	1.597	\pm	0.073

Table S4: Concentration of THMs and bromine incorporation factor (BIF) of coagulated/filtered and treated algae-laden water.

Processes	Time			•		Conc	centration	ı (μg/L)		•	•			BIF - THMs 0.139
	(min)		CF		BDe	CM		DBC	CM		BF			
VUV	0	246.10	±	5.51	41.80	±	1.26	7.34	±	0.25	0.16	±	0.01	
	10	190.97	\pm	21.17	35.83	\pm	1.26	7.58	\pm	0.93	0.24	\pm	0.02	0.159
	30	175.41	\pm	2.03	35.80	\pm	1.19	7.60	\pm	0.92	0.22	\pm	0.01	0.171
	60	133.29	\pm	0.18	33.00	\pm	0.53	8.06	\pm	0.38	0.26	\pm	0.01	0.208
VUV/PS	0	246.10	±	5.51	41.80	±	1.26	7.34	±	0.25	0.16	±	0.01	0.139
5 mg/L	10	192.48	\pm	4.04	38.42	\pm	1.52	7.55	\pm	0.49	0.25	\pm	0.03	0.165
	30	221.60	\pm	0.00	46.95	\pm	7.06	8.59	\pm	0.54	0.27	\pm	0.00	0.170
	60	127.37	±	4.61	32.39	±	2.82	8.05	±	0.85	0.29	±	0.07	0.213
VUV/PS	0	246.10	±	5.51	41.80	±	1.26	7.34	±	0.25	0.16	±	0.01	0.139
50 mg/L	10	159.63	\pm	25.77	42.47	\pm	11.05	6.25	\pm	2.17	0.22	\pm	0.00	0.198
	30	160.54	\pm	23.77	32.28	\pm	4.76	6.33	\pm	0.56	0.21	\pm	0.00	0.166
	60	139.28	\pm	0.00	33.33	\pm	3.26	6.92	\pm	0.37	0.24	\pm	0.01	0.194
UV	0	246.10	±	5.51	41.80	±	1.26	7.34	±	0.25	0.16	±	0.01	0.139
	10	228.99	\pm	45.67	41.44	\pm	0.00	7.42	\pm	0.00	0.14	\pm	0.03	0.148
	30	237.32	\pm	10.42	37.33	\pm	0.48	6.67	\pm	0.30	0.15	\pm	0.02	0.131
	60	224.54	±	21.53	38.68	\pm	1.95	7.28	±	0.05	0.18	±	0.00	0.143
UV/PS	0	246.10	±	5.51	41.80	±	1.26	7.34	±	0.25	0.16	±	0.01	0.139
5 mg/L	10	199.02	\pm	19.19	35.77	\pm	0.30	7.38	\pm	0.49	0.21	\pm	0.05	0.152
	30	197.58	\pm	0.00	31.59	\pm	5.90	6.53	\pm	0.95	0.18	\pm	0.05	0.137
	60	175.09	\pm	12.40	32.82	\pm	3.10	6.74	\pm	0.55	0.21	\pm	0.03	0.157
UV/PS	0	246.10	±	5.51	41.80	±	1.26	7.34	±	0.25	0.16	±	0.01	0.139
50 mg/L	10	197.77	\pm	11.44	39.42	\pm	7.50	6.72	\pm	1.08	0.18	\pm	0.02	0.159
	30	203.32	\pm	2.09	39.68	\pm	1.69	6.72	\pm	0.15	0.17	\pm	0.00	0.156
	60	201.76	\pm	24.27	40.67	\pm	0.19	7.14	\pm	0.02	0.19	\pm	0.01	0.162

S. Soontharo et al., "Reduction of Carbonaceous and Nitrogenous Disinfection Byproduct Precursors from Coagulated/Filtered Algaeladen Water: Comparison of Vacuum Ultraviolet and Ultraviolet Processes with and without Persulfate Activation."



Table S5: Concentration of HANs and bromine incorporation factor (BIF) of coagulated/filtered and treated

Processes	Time			·	·			Concen	tratio	n (μg/L)				·		·	BIF -
	(min)	-	TCAN	N	MCAN]	DCA	V	DBAN			MBAN			HANs
VUV	0	0.113	±	0.018	0.297	±	0.034	3.784	±	0.114	0.101	±	0.011	0.311	±	0.015	0.087
	10	0.115	\pm	0.013	0.175	\pm	0.014	3.241	\pm	0.796	0.048	\pm	0.002	0.311	\pm	0.037	0.089
	30	0.156	\pm	0.017	0.156	\pm	0.015	3.049	\pm	0.937	0.037	\pm	0.003	0.325	\pm	0.010	0.094
	60	0.119	±	0.017	0.141	\pm	0.001	3.033	\pm	0.632	0.024	\pm	0.001	0.340	\pm	0.018	0.095
VUV/PS	0	0.113	±	0.018	0.297	\pm	0.034	3.784	±	0.114	0.101	±	0.011	0.311	±	0.015	0.087
5 mg/L	10	0.193	\pm	0.017	0.157	\pm	0.014	2.450	\pm	0.379	0.043	\pm	0.000	0.304	\pm	0.026	0.110
	30	0.197	\pm	0.053	0.203	\pm	0.027	3.824	\pm	0.372	0.040	\pm	0.007	0.362	\pm	0.021	0.084
	60	0.212	\pm	0.004	0.210	±	0.013	3.081	±	0.012	0.024	±	0.004	0.400	±	0.001	0.104
VUV/PS	0	0.113	±	0.018	0.297	\pm	0.034	3.784	±	0.114	0.101	±	0.011	0.311	±	0.015	0.087
50 mg/L	10	0.250	\pm	0.000	0.152	\pm	0.001	3.081	\pm	0.184	0.043	\pm	0.013	0.326	\pm	0.039	0.095
	30	0.274	\pm	0.064	0.167	\pm	0.020	3.007	\pm	0.510	0.033	\pm	0.001	0.356	\pm	0.101	0.101
	60	0.291	±	0.055	0.128	\pm	0.001	2.991	\pm	0.841	0.015	\pm	0.001	0.330	\pm	0.059	0.092
UV	0	0.113	±	0.018	0.297	\pm	0.034	3.784	±	0.114	0.101	±	0.011	0.311	±	0.015	0.087
	10	0.094	\pm	0.001	0.245	\pm	0.017	3.672	\pm	0.170	0.073	\pm	0.006	0.295	\pm	0.035	0.081
	30	0.091	\pm	0.006	0.208	\pm	0.007	3.375	\pm	0.243	0.059	\pm	0.012	0.260	\pm	0.013	0.077
	60	0.086	±	0.001	0.195	\pm	0.013	3.463	\pm	0.153	0.068	\pm	0.002	0.303	\pm	0.027	0.087
UV/PS	0	0.113	±	0.018	0.297	\pm	0.034	3.784	±	0.114	0.101	±	0.011	0.311	±	0.015	0.087
5 mg/L	10	0.109	\pm	0.021	0.237	\pm	0.001	3.464	\pm	0.270	0.075	\pm	0.036	0.360	\pm	0.020	0.099
	30	0.156	\pm	0.065	0.197	\pm	0.009	3.335	\pm	0.137	0.071	\pm	0.003	0.345	\pm	0.003	0.099
	60	0.143	±	0.027	0.212	\pm	0.046	3.176	\pm	0.319	0.071	\pm	0.017	0.299	\pm	0.019	0.093
UV/PS	0	0.113	±	0.018	0.297	±	0.034	3.784	±	0.114	0.101	±	0.011	0.311	±	0.015	0.087
50 mg/L	10	0.099	\pm	0.014	0.149	\pm	0.026	3.075	\pm	0.264	0.044	\pm	0.013	0.282	\pm	0.025	0.086
	30	0.103	\pm	0.005	0.128	\pm	0.002	3.112	\pm	0.001	0.047	\pm	0.001	0.213	\pm	0.002	0.070
	60	0.094	\pm	0.033	0.139	\pm	0.002	3.037	\pm	0.110	0.054	\pm	0.022	0.270	\pm	0.001	0.087

Table S6: The ratio of each THM to the respective WHO guideline value.

Processes	Reaction Time		Ratio ^a								
	(min)	CF	BDCM	DBCM	BF	_					
VUV	0	0.820	0.697	0.073	0.002	1.592					
	10	0.637	0.597	0.076	0.002	1.312					
	30	0.585	0.597	0.076	0.002	1.260					
	60	0.444	0.550	0.081	0.003	1.077					
VUV/PS	0	0.820	0.697	0.073	0.002	1.592					
5 mg/L	10	0.642	0.640	0.075	0.003	1.360					
	30	0.739	0.782	0.086	0.003	1.610					
	60	0.425	0.540	0.080	0.003	1.048					
VUV/PS	0	0.820	0.697	0.073	0.002	1.592					
50 mg/L	10	0.532	0.708	0.062	0.002	1.305					
	30	0.535	0.538	0.063	0.002	1.139					
	60	0.464	0.556	0.069	0.002	1.091					
UV	0	0.820	0.697	0.073	0.002	1.592					
	10	0.763	0.691	0.074	0.001	1.530					
	30	0.791	0.622	0.067	0.001	1.481					
	60	0.748	0.645	0.073	0.002	1.468					
UV/PS	0	0.820	0.697	0.073	0.002	1.592					
5 mg/L	10	0.663	0.596	0.074	0.002	1.335					
	30	0.659	0.526	0.065	0.002	1.252					
	60	0.584	0.547	0.067	0.002	1.200					
UV/PS	0	0.820	0.697	0.073	0.002	1.592					
50 mg/L	10	0.659	0.657	0.067	0.002	1.385					
	30	0.678	0.661	0.067	0.002	1.408					
	60	0.673	0.678	0.071	0.002	1.424					

Note:

 $[^]a$ The ratio of each THM to the respective WHO guideline value (CF = 300 μ g/L, BDCM = 60 μ g/L, DBCM = 100 μ g/L, and BF = 100 $\mu g/L).$ b The sum of the ratio of the concentration of each to its respective guideline value should not exceed 1 [4].



References

- [1] R. O. Rahn, J. Bolton, and M. I. Stefan, "The Iodide/Iodate actinometer in UV disinfection: determination of the fluence rate distribution in UV reactors," *Photochemistry and Photobiology*, vol. 82, p. 611, 2006, doi: 10.1562/2005-06-10rn-570.
- [2] J. Zhang, H. Zhang, X. Liu, F. Cui, and Z. Zhao, "Efficient reductive and oxidative decomposition of haloacetic acids by the vacuum-ultraviolet/ sulfite system," *Water Research*, vol. 210, p. 117974, 2022, doi: 10.1016/j.watres.2021.117974.
- [3] U.S. Environmental Protection Agency, Method 551.1: Determination of Chlorination Disinfection Byproducts, Chlorinated Solvents, and Halogenated Pesticides/Herbicides in Drinking Water by Liquid-Liquid Extraction and Gas Chromatography with Electron-Capture Detection, Revision 1. Cincinnati, OH, USA: U.S. Environmental Protection Agency, 1995.
- [4] World Health Organization, Guidelines for Drinking-water Quality: Fourth Edition Incorporating the First Addendum, 4th ed. Geneva, Switzerland: World Health Organization, 2017.